PNAS
www.pnas.org

Supplementary Information for

Hypoxia induces a time and tissue-specific response that elicits inter-tissue circadian clock misalignment

Gal Manella, Rona Aviram, Nityanand Bolshette, Sapir Muvkadi, Marina Golik, David F. Smith and Gad Asher

Corresponding Author: Gad Asher, gad.asher@weizmann.ac.il

This PDF file includes:

Other supplementary materials for this manuscript include the following:

Supplementary Materials and Methods

Contact for reagent and resource sharing

Further information and requests for resources and reagents should be directed to and will be fulfilled by the Lead Contact, Gad Asher (gad.asher@weizmann.ac.il)

Animals

All animal experiments and procedures were conducted in conformity with the Weizmann Institute Animal Care and Use Committee (IACUC) guidelines. Three to four months-old male wild type C57BL/6 mice (Envigo), *Per1,2*$^{-/-}$mice (1) back crossed to C57BL/6 and PER2::LUCIFERASE mice (2) were used. *Alb-Cre*$^{+}$ *Bmal1*$^{fl/fl}$ were generated by crossing Alb-Cre^{+} mice (Jackson Laboratories) with *Bmal*$^{fl/fl}$ mice (3), (Jackson Laboratories). Animals were housed in an SPF animal facility, at ambient temperature of ≈22^{0}C, under a 12 h light-dark regimen (LD) and fed *ad libitum*, unless indicated otherwise. Experiments under constant dark (DD) were performed on the second day of DD, following regular LD regimen. Mice were euthanized by cervical dislocation.

Hypoxia treatment

The sustained hypoxia treatment described in Fig. 1-4, was conducted using a home-made constant flow system. The system is constructed from a standard, sealed-top cage (Techniplast), connected by tubing to a gas cylinder of either 6% O_2 + 94% N_2 mixture, or 21% O_2 + 79% N_2 (synthetic air) as a control (Gordon Gas, IL). During the hypoxic

experiments mice were housed in the dedicated cages, and the indicated gas mixtures were delivered in constant flow rate of 3.5 LPM for 4 h.

The sustained and intermittent hypoxia treatment described in Fig. 6 were conducted using the $VelO_2x$ *in vivo* hypoxia system (Baker Co.). This system produces high-rate changes in oxygen concentration in a closed chamber, therefore enabling implementation of intermittent hypoxia protocols. The sustained hypoxia protocol that was used: 5' of 15% O_2; 10' of 10% O_2; 3h 45' of 6.5% O_2. The intermittent hypoxia protocol that was used: ≈30 hypoxic cycles per hour for total of 4 h, where each cycle consists of approximately 30'' of down-slope, 30'' of 6% O_2, 30'' of up-slope, and 30'' of 21% O_2.

RNA extraction

Tissues were snap-frozen in liquid nitrogen immediately after dissection and stored at −80°C till used. For RNA extraction, the tissues were soaked in TRI-reagent (Sigma) and were homogenized by dispenser (IKA-T18), and then proceeded by a standard TRI-reagent based RNA extraction protocol. RNA concentration was determined using NanoDrop™ 2000 Spectrophotometer (Thermo Fisher Scientific). RNA quality was validated using 2200 TapeStation (Agilent).

MARS-seq library preparation and sequencing

We used a derivation of the MARS-seq as described (4), originally developed for single-cell RNA-seq to produce expression libraries, and exclusively sequencing the 3'-end of the transcripts. The prepared MARS-seq libraries were sequenced with high-output 75 bp kit (FC-404-2005, Illumina) on NextSeq 500/550 Illumina sequencer.

RNA-seq data processing

Processing of raw sequencing data into read counts was performed via the User-friendly Transcriptome Analysis Pipeline (UTAP) (5).

In short, Reads were trimmed using cutadapt (6) and mapped to genome (/shareDB/iGenomes/Mus_musculus/UCSC/mm10/Sequence/STAR_index) using STAR (7) (default parameters). The pipeline quantifies the genes annotated in RefSeq (that have expanded with 1000 bases toward 5' edge and 100 bases toward 3' bases). Counting was done using htseq-count (union mode) (8).

RNA-seq statistical analysis

The statistical analysis was performed separately for each tissue. Only genes with at least 2 reads in at least two samples were included in the analysis. The data was normalized based on the 'EdgeR' package normalization method (9). Statistical analysis of differentially expressed genes in the different contrasts was performed by the stage-wise approach, using the R package 'StageR' (10). In principle, stage-wise analysis divides the testing of multiple hypotheses (contrasts) on multiple genes into two stages: first, it screens for an omnibus hypothesis and apply false-discovery correction on this test's results. Then, only genes that passed the screening test are tested for the specific contrasts (i.e. the confirmation hypotheses). A family-wise error rate (FWER) method is applied to correct for the multiple hypotheses in the second stage. The stage-wise analysis allows an enhanced power in multiple testing of interaction effects without a major influence on main effects. To test the screening hypothesis (i.e. no difference in either of the relevant

contrasts) we used the F-test from the 'limma' package (11) on a fitting model with the following contrasts: ZT8 21% vs. ZT20 21%; ZT8 21% vs ZT8 6%; ZT20 21% vs ZT20 6%; and interaction between oxygen level and ZT. An OFDR (Overall False Discovery Rate) was calculated from the F-test's p-values for each gene by the Benjamini-Hochberg method. Only genes with OFDR < 0.05 were tested for the confirmation hypotheses, i.e. for significance in each of the specific contrasts above. The "holm" FWER method was applied per gene, and adjusted p-value < 0.05 for a specific hypothesis was considered significant. A similar scheme was performed for the analysis of the RNA-seq from WT and Per1,2$^{-/-}$ livers. Raw and normalized counts, and statistics for all genes and conditions are detailed in Datasets S1-S2.

Motif analysis

Motif enrichment analysis was preformed using the Fast Gene Set Enrichment Analysis method (FGSEA) (12, 13). Gene ranking was based on the fold-change of the genes in each contrast. The motif annotation was retrieved from the MSigDB (14) C3 Transcription Factor Targets collection, with is based on (15). The full results appear in Dataset S7.

Pathway enrichment analysis

MSigDB pathway enrichment analysis (14) was performed using the 'ClusterProfiler' R package (16), with p-value < 0.05 and Benjamini-Hochberg q-value < 0.2. The "C2 Canonical Pathways" (c2.cp.v6.2.symbols.gmt) collection was used. Mouse gene symbols were converted to human symbols using 'biomaRt' (17). The full lists of significant gene sets are supplied in Dataset S8.

Hierarchical clustering

Clustering of time-dependent responsive genes in each of the tissues (Fig. 1D) was performed by hierarchical clustering with "Euclidean" distance measure and "complete" agglomeration method, and a fixed cluster number of 8.

Clustering of enriched pathways (Fig. S2, S3B) was performed with "binary" distance and the "single" method, on a table of significant indicators in each comparison (i.e. 1=significant, 0=non-significant).

Quantitative PCR

Synthesis of cDNA was performed using qScript cDNA SuperMix (Quanta Biosciences). Real-time quantitative PCR measurements were performed using SYBR green or TaqMan probes with LightCycler II machine (Roche) and normalized to the geometrical mean of two housekeeping genes: *Rplp0* and *Tbp*. Primers and probes are detailed in Table S1.

Protein extraction

Tissues were snap-frozen in liquid nitrogen immediately after dissection and stored at −80°C until used. For total protein extraction, tissues were homogenized by a dispenser (IKA-T18) in ice-cold RIPA buffer (150 mM NaCl, 1% NP-40, 0.5% Na-deoxycholate, 0.1% SDS, 50 mM Tris-Hcl pH 8, and 1 mM dithiothreitol). The extracts were centrifuged at 13,000 rpm for 15 min at 4°C.

Nuclei were isolated by density sucrose gradient as previously described (18). For liver nuclei, the entire liver was used. For lung and kidney, due to technical reasons, to ensure

efficient nuclear isolation we used pools from 4 biological replicates. Subsequently, nuclear proteins were extracted by adding 1:1 NUN buffer (50mM HEPES pH=7.6, 0.6M NaCl, 2% NP-40, 2M Urea), (19).

All buffers were supplemented with: protease inhibitors cocktail (1 mM N-(a-aminoethyl) benzene-sulfonyl fluoride, 40 mM bestatin, 15 mM E65, 20 mM leupeptin, and 15 mM pepstatin) (Sigma), PMSF (1:200), Vannadate (1:500), DTT (1:1000), NaF (1:1000).

Immunoblot analysis

Protein concentration was determined by the Bradford assay (Bio-Rad), and equalized between samples. Then, samples were heated at 95°C for 5 min in Laemmli sample buffer and analyzed by SDS-PAGE and immunoblot. Antibodies that were used: Rabbit anti-CLOCK, anti-ARNTL, anti-PER2 (Asher et al., 2010), anti-CRY1 (Bethyl), anti-p-NR1D1 (Cell Signaling Technology), and Mouse anti-HIF1A (Santa Cruz), anti-TUBULIN and anti-U2AF (Sigma).

PER2::LUC organotypic slices biluminescence recording

Organotypic slices bioluminescence assay was performed as previously described (2). In short, mice were euthanized by cervical dislocation and their organs were dissected and placed in HBSS buffer (Gibco). The different tissues were sliced to pieces of about 1mm^2 area, each transferred into a 3.5cm culture dish supplemented with 1ml of culture buffer (High Glucose DMEM without phenol red (Gibco)), supplemented with 100nM D-Luciferin (Promega), 1:20000 DMSO (Sigma), 100units/mL penicillin and 100mg/mL streptomycin (Biological Industries)). The plates were sealed with parafilm (Bemis) and

incubated in a LumiCycle32 (Actimetrics), in 37°C, 5% CO_2. Bioluminescence was recorded for at least three consecutive days.

Bioluminescence recording analysis

Bioluminescence recordings were extracted using the LumiCycle Analysis software (Actimatrics). Subsequent analyses were performed using MATLAB (Mathworks). The time dimension was realigned to correspond to the ZT of the animal. The data was de-trended by normalizing it to a 48 h running average trend. Peaks in the data were detected by smoothing the data with a 2 h running average and then applying the Matlab '*findpeaks'* function with a minimal peak width of 200 min. The first peak after CT30 was considered as the phase marker for each trajectory. Circular mean and variance calculations, and Watson-Williams test were performed using the MATLAB CircStat toolbox (20).

***Ex vivo* hypoxia and PTC construction**

Tissues were dissected and incubated as described above for luminescence recording. Then, the oxygen levels in the treatment incubator were decreased to 2.5% for 4 h, using an O_2/N_2 controller system (COY Laboratories). Unperturbed slices from the same mice were incubated in a control incubator under constant normoxia. After de-trending and peak detection, the first peak post treatment was compared to the respective peak in the control for each biological replicate, to construct a PTC.

Cosine fit for phase determination

Cosine fit for the analysis of phases in the time-course experiment (Fig. 6D) was performed using the MATLAB 'fit' function with the model: $y=b+a\cdot\cos(2\pi x/24 - c)$, where the parameter c represent the phase in radian, and the period length was predetermined as 24 h. The fit was performed on each batch separately (the experiment was repeated 3 times, in each one mouse per time-point per condition was used), as well as the phase differences per gene. The data for fitting obtained from the last 22 h of the experiment, to avoid interruption from immediate responses to the hypoxia and re-oxygenation.

Computation and statistics

All the statistical analysis was performed by either R 3.5.1 or MATLAB R2017b. specific information on sample sizes, statistical significance and variance measures is provided in the relevant figure legends.

Supplementary Figures

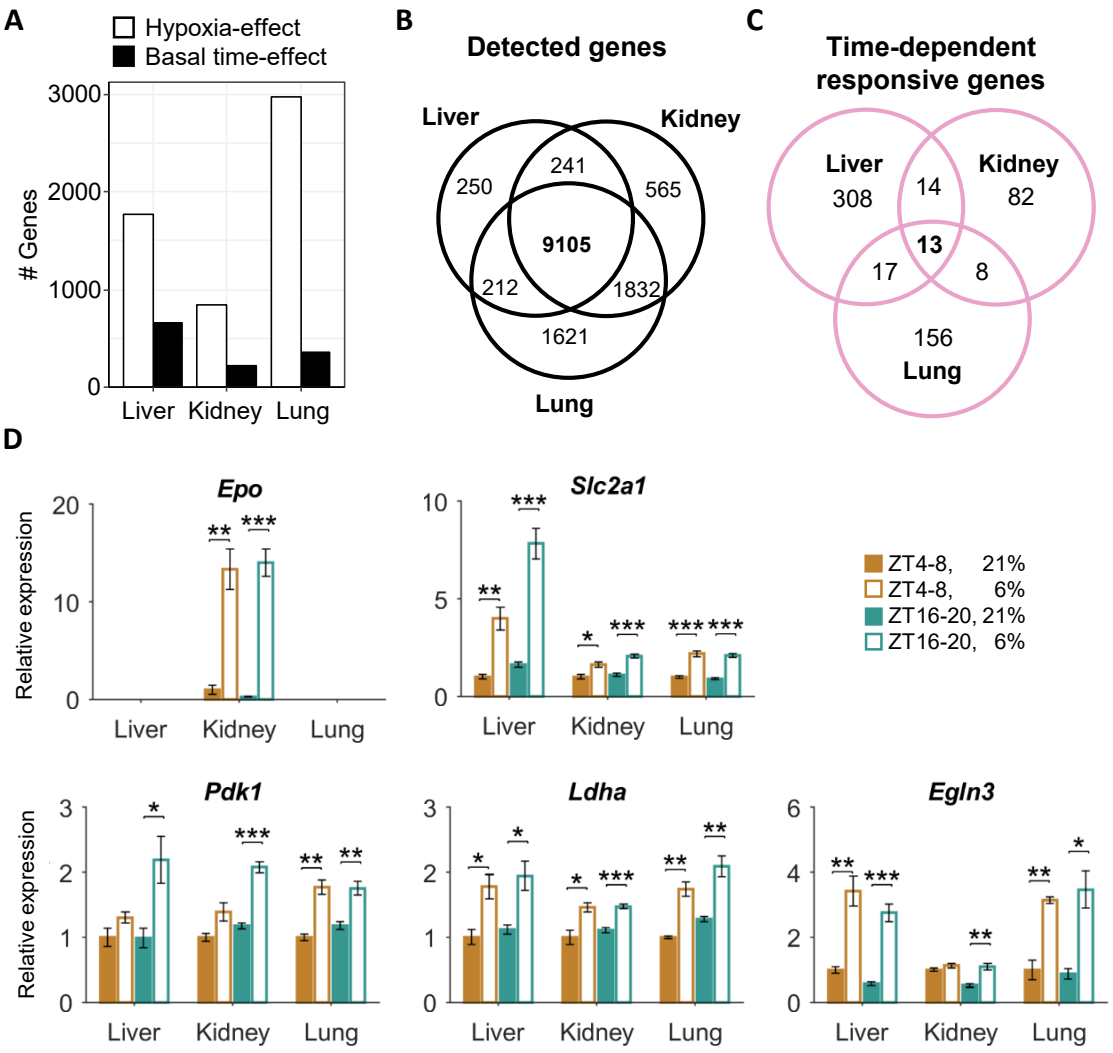

E

Response in:	Top predicted transcription factors
Liver ZT4-8	ATF, CREB, CREBP1, SRF, ATF, HIF1, BACH2, ATF3, CEBP, AP1
Liver ZT16-20	ATF, CREB, CREBP1, SRF, ATF, HIF1, BACH2, ATF3, CEBP, AP1
Kidney ZT4-8	CREB, CREBP, BACH2, ATF4, E4F1, NFkB
Kidney ZT16-20	CREB, CREBP1, STAT5A, ATF3, SRF, BACH2, ATF4, PAX3, E4F1, HMEF2
Lung ZT4-8	ATF, CREB, CREBP1/cJUN, CREBP1, SRF, STAT5A, ATF3, ATF4, E4F1, AP4, PAX3
Lung ZT16-20	ATF, CREB, CREBP, SRF, AP1, ETS, BACH2, BACH1, ATF3, ATF4, E4F1

Figure S1. The transcriptional response to hypoxia is time- and tissue-dependent.

Mice were exposed to 4 h of either hypoxia (6% O_2) or normoxia (21% O_2), at the light (ZT4-8) or dark phase (ZT16-20). Animals were sacrificed, tissues harvested, and RNA was prepared and sequenced.

(A) Number of genes that significantly responded to hypoxia (including response in either of the time points or a significant interaction), or had a significant basal-time effect (i.e. a difference between the time points in the normoxia condition), (Stage-wise analysis, OFDR < 0.05, adjusted p-value < 0.05, n=4 per condition).

(B) A Venn diagram representing the number of detected genes (at least two reads in two samples) for each tissue.

(C) A Venn diagram representing the number of genes that significantly responded to hypoxia in a time-dependent manner in each tissue (i.e. significant interaction, same criteria as in (**A**)), (see Dataset S4 for gene lists).

(D) Quantitative PCR analysis of representative canonical hypoxia-responsive genes. *Epo* was not well detected in samples from liver and lung and therefore is not included for these tissues (mean ± SE, n=4 per condition; *P<0.05, **P<0.01, ***P<0.001, two-sample Student's t-test).

(E) The top over-represented transcription factors in each comparison, based on motif enrichment analysis (FDR < 0.05). See Dataset S7 for the full details.


PID_VEGFR1_2_PATHWAY
REACTOME_ACTIVATED_TLR4_SIGNALLING
REACTOME_UNFOLDED_PROTEIN_RESPONSE
REACTOME_TRIGLYCERIDE_BIOSYNTHESIS
REACTOME_TRANSCRIPTIONAL_REGULATION_OF_WHITE_ADIPOCYTE_DIFFERENTIATION
REACTOME_REGULATION_OF_MRNA_STABILITY_BY_PROTEINS_THAT_BIND_AU_RICH_ELEMENTS
REACTOME_PERK_REGULATED_GENE_EXPRESSION
REACTOME_FATTY_ACYL_COA_BIOSYNTHESIS
REACTOME_DESTABILIZATION_OF_MRNA_BY_BRF1
REACTOME_CHOLESTEROL_BIOSYNTHESIS
REACTOME_ACTIVATION_OF_GENES_BY_ATF4
PID_IFNG_PATHWAY
KEGG_RETINOL_METABOLISM
KEGG_PEROXISOME
KEGG_INSULIN_SIGNALING_PATHWAY
KEGG_ALANINE_ASPARTATE_AND_GLUTAMATE_METABOLISM
KEGG_FRUCTOSE_AND_MANNOSE_METABOLISM
REACTOME_NUCLEAR_RECEPTOR_TRANSCRIPTION_PATHWAY
REACTOME_COLLAGEN_FORMATION
REACTOME_CIRCADIAN_REPRESSION_OF_EXPRESSION_BY_REV_ERBA
REACTOME_BILE_SALT_AND_ORGANIC_ANION_SLC_TRANSPORTERS
PID_AR_TF_PATHWAY
KEGG_P53_SIGNALING_PATHWAY
KEGG_NOTCH_SIGNALING_PATHWAY
BIOCARTA_PLATELETAPP_PATHWAY
BIOCARTA_VITCB_PATHWAY
ST_TUMOR_NECROSIS_FACTOR_PATHWAY
ST_JNK_MAPK_PATHWAY
REACTOME_SYNTHESIS_OF_PE
REACTOME_SYNTHESIS_OF_PC
REACTOME_PROCESSING_OF_INTRONLESS_PRE_MRNAS
REACTOME_GLYCOLYSIS
REACTOME_GLYCEROPHOSPHOLIPID_BIOSYNTHESIS
PID_ERA_GENOMIC_PATHWAY
KEGG_CYSTEINE_AND_METHIONINE_METABOLISM
BIOCARTA_MTA3_PATHWAY
BIOCARTA_PDGF_PATHWAY
SIG_PIP3_SIGNALING_IN_CARDIAC_MYOCTES
SA_CASPASE_CASCADE
REACTOME_SIGNALING_BY_THE_B_CELL_RECEPTOR_BCR
REACTOME_SIGNALING_BY_SCF_KIT
REACTOME_SIGNALING_BY_NOTCH4
REACTOME_SIGNALING_BY_NOTCH3
REACTOME_SIGNALING_BY_NOTCH2
REACTOME_POST_CHAPERONIN_TUBULIN_FOLDING_PATHWAY
REACTOME_NUCLEOTIDE_BINDING_DOMAIN_LEUCINE_RICH_REPEAT_CONTAINING_RECEPTOR_NLR_SIGNALING_PATHWAYS
REACTOME_INTERFERON_GAMMA_SIGNALING
REACTOME_FORMATION_OF_TUBULIN_FOLDING_INTERMEDIATES_BY_CCT_TRIC
REACTOME_DOWNSTREAM_SIGNALING_EVENTS_OF_B_CELL_RECEPTOR_BCR
REACTOME_CYTOSOLIC_TRNA_AMINOACYLATION
REACTOME_APOPTOSIS
REACTOME_AMINO_ACID_TRANSPORT_ACROSS_THE_PLASMA_MEMBRANE
PID_TAP63_PATHWAY
PID_RXR_VDR_PATHWAY
PID_PRL_SIGNALING_EVENTS_PATHWAY
PID_IGF1_PATHWAY
PID_FAK_PATHWAY
PID_EPO_PATHWAY
KEGG_FOCAL_ADHESION
KEGG_ADIPOCYTOKINE_SIGNALING_PATHWAY
BIOCARTA_PTEN_PATHWAY
BIOCARTA_CASPASE_PATHWAY
BIOCARTA_INTEGRIN_PATHWAY
WNT_SIGNALING
REACTOME_TRAF6_MEDIATED_IRF7_ACTIVATION
REACTOME_TRAF6_MEDIATED_INDUCTION_OF_NFKB_AND_MAP_KINASES_UPON_TLR7_8_OR_9_ACTIVATION
REACTOME_TRAF3_DEPENDENT_IRF_ACTIVATION_PATHWAY
REACTOME_NFKB_AND_MAP_KINASES_ACTIVATION_MEDIATED_BY_TLR4_SIGNALING_REPERTOIRE
REACTOME_NEGATIVE_REGULATORS_OF_RIG_I_MDA5_SIGNALING
REACTOME_MYD88_MAL_CASCADE_INITIATED_ON_PLASMA_MEMBRANE
REACTOME_MAPK_TARGETS_NUCLEAR_EVENTS_MEDIATED_BY_MAP_KINASES
REACTOME_MAP_KINASE_ACTIVATION_IN_TLR_CASCADE
PID_NETRIN_PATHWAY
PID_MAPK_TRK_PATHWAY
PID_IL12_2PATHWAY
PID_ECADHERIN_STABILIZATION_PATHWAY
PID_ECADHERIN_NASCENT_AJ_PATHWAY
PID_BETA_CATENIN_DEG_PATHWAY
KEGG_WNT_SIGNALING_PATHWAY
KEGG_TIGHT_JUNCTION
BIOCARTA_RANKL_PATHWAY
BIOCARTA_P53HYPOXIA_PATHWAY
BIOCARTA_MAPK_PATHWAY
BIOCARTA_IL6_PATHWAY
BIOCARTA_IL1R_PATHWAY
BIOCARTA_ATM_PATHWAY
BIOCARTA_ETS_PATHWAY
PID_FRA_PATHWAY
PID_MYC_REPRESS_PATHWAY
PID_CIRCADIAN_PATHWAY
PID_SMAD2_3NUCLEAR_PATHWAY
PID_RET_PATHWAY
REACTOME_PPARA_ACTIVATES_GENE_EXPRESSION
REACTOME_METABOLISM_OF_LIPIDS_AND_LIPOPROTEINS
REACTOME_FATTY_ACID_TRIACYLGLYCEROL_AND_KETONE_BODY_METABOLISM
PID_HNF3B_PATHWAY
PID_HIF2PATHWAY
KEGG_PPAR_SIGNALING_PATHWAY
BIOCARTA_PPARA_PATHWAY
BIOCARTA_TOLL_PATHWAY
BIOCARTA_ARENRF2_PATHWAY
PID_P38_MKK3_6PATHWAY
REACTOME_BMAL1_CLOCK_NPAS2_ACTIVATES_CIRCADIAN_EXPRESSION
REACTOME_CIRCADIAN_CLOCK
KEGG_CIRCADIAN_RHYTHM_MAMMAL
PID_P53_DOWNSTREAM_PATHWAY
PID_IL6_7_PATHWAY
PID_HIF1_TFPATHWAY
PID_AP1_PATHWAY
PID_ATF2_PATHWAY
PID_REG_GR_PATHWAY
REACTOME_RORA_ACTIVATES_CIRCADIAN_EXPRESSION
PID_NFAT_TFPATHWAY
KEGG_PATHWAYS_IN_CANCER
REACTOME_TRIF_MEDIATED_TLR3_SIGNALING
REACTOME_RIG_I_MDA5_MEDIATED_INDUCTION_OF_IFN_ALPHA_BETA_PATHWAYS
REACTOME_PREFOLDIN_MEDIATED_TRANSFER_OF_SUBSTRATE_TO_CCT_TRIC
REACTOME_CYTOKINE_SIGNALING_IN_IMMUNE_SYSTEM
PID_RHOA_PATHWAY
PID_PDGFRB_PATHWAY
PID_MTOR_4PATHWAY
PID_MET_PATHWAY
PID_IL2_1PATHWAY
PID_HIV_NEF_PATHWAY
PID_ERBB1_DOWNSTREAM_PATHWAY
PID_CD40_PATHWAY
PID_CASPASE_PATHWAY
KEGG_SMALL_CELL_LUNG_CANCER
KEGG_LEUKOCYTE_TRANSENDOTHELIAL_MIGRATION
BIOCARTA_TNFR2_PATHWAY
BIOCARTA_STRESS_PATHWAY
BIOCARTA_IL2RB_PATHWAY
BIOCARTA_DEATH_PATHWAY
BIOCARTA_HIVNEF_PATHWAY
KEGG_MAPK_SIGNALING_PATHWAY
KEGG_PATHOGENIC_ESCHERICHIA_COLI_INFECTION
BIOCARTA_KERATINOCYTE_PATHWAY
BIOCARTA_CDMAC_PATHWAY
ST_P38_MAPK_PATHWAY
Liver
Kidney
Lung
Gene Ratio
0.1
0.08
0.06
0.04
0.02
0
ZT4-8, 21% vs. 6%
ZT16-20, 21% vs. 6%

Figure S2. Pathway enrichment analysis of the response to hypoxia across times-of-day and tissues

MSigDB Canonical Pathways enrichment analysis for the responsive genes in each experimental comparison (hypergeometric test, p-value<0.05, q-value<0.2; white indicates a non-significant enrichment in the specific cell; Gene Ratio is the ratio between responsive gene set members and the total number of responsive genes in the comparison). See Dataset S8 for extra details.

A

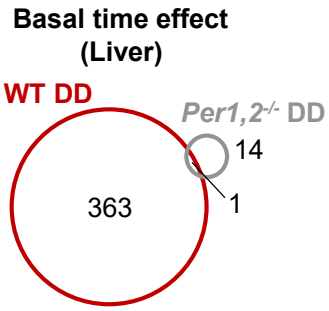
Basal time effect
(Liver)
WT DD
Per1,2-/- DD
14
363
1

B


REACTOME_UNFOLDED_PROTEIN_RESPONSE
REACTOME_NUCLEAR_RECEPTOR_TRANSCRIPTION_PATHWAY
REACTOME_DIABETES_PATHWAYS
REACTOME_BIOLOGICAL_OXIDATIONS
REACTOME_ALPHA_LINOLENIC_ACID_ALA_METABOLISM
KEGG_RETINOL_METABOLISM
KEGG_BIOSYNTHESIS_OF_UNSATURATED_FATTY_ACIDS
KEGG_LINOLEIC_ACID_METABOLISM
REACTOME_TRIGLYCERIDE_BIOSYNTHESIS
REACTOME_METABOLISM_OF_AMINO_ACIDS_AND_DERIVATIVES
REACTOME_FATTY_ACYL_COA_BIOSYNTHESIS
REACTOME_CHOLESTEROL_BIOSYNTHESIS
PID_RXR_VDR_PATHWAY
PID_P38_MKK3_6PATHWAY
PID_P38_GAMMA_DELTA_PATHWAY
PID_IL6_7_PATHWAY
PID_E2F_PATHWAY
KEGG_TERPENOID_BACKBONE_BIOSYNTHESIS
KEGG_STEROID_BIOSYNTHESIS
KEGG_CYSTEINE_AND_METHIONINE_METABOLISM
KEGG_ADIPOCYTOKINE_SIGNALING_PATHWAY
BIOCARTA_TOLL_PATHWAY
BIOCARTA_NTHI_PATHWAY
BIOCARTA_P53_PATHWAY
REACTOME_TRANSCRIPTIONAL_REGULATION_OF_WHITE_ADIPOCYTE_DIFFERENTIATION
REACTOME_PPARA_ACTIVATES_GENE_EXPRESSION
REACTOME_PHASE1_FUNCTIONALIZATION_OF_COMPOUNDS
REACTOME_METABOLISM_OF_LIPIDS_AND_LIPOPROTEINS
REACTOME_FATTY_ACID_TRIACYLGLYCEROL_AND_KETONE_BODY_METABOLISM
REACTOME_CYTOCHROME_P450_ARRANGED_BY_SUBSTRATE_TYPE
REACTOME_CIRCADIAN_CLOCK
REACTOME_BMAL1_CLOCK_NPAS2_ACTIVATES_CIRCADIAN_EXPRESSION
PID_SMAD2_3NUCLEAR_PATHWAY
PID_P53_DOWNSTREAM_PATHWAY
PID_HNF3B_PATHWAY
PID_HIF2PATHWAY
PID_HIF1_TFPATHWAY
PID_FRA_PATHWAY
PID_ATF2_PATHWAY
PID_AP1_PATHWAY
KEGG_PPAR_SIGNALING_PATHWAY
BIOCARTA_NUCLEARRS_PATHWAY
BIOCARTA_PPARA_PATHWAY
Gene Ratio
0.1
0.08
0.06
0.04
0.02
0
WT
Per1,2-/-

Figure S3. Basal-time effect and hypoxia response in liver gene expression is *Per1,2*-dependent.

Wild-type (WT) and *Per1,2*$^{-/-}$ mice were housed in constant dark for two consecutive days and exposed to 4 h of either hypoxia (6% O2) or control normoxia (21% O2), at the subjective light (CT4-8) or dark phase (CT16-20). Animals were sacrificed, livers harvested, and RNA was prepared and sequenced.

(A) A Venn diagram representing the number of genes with a significant basal-time effect (i.e. control normoxia), in livers of WT or *Per1,2*$^{-/-}$ mice (see Dataset S6 for gene lists)

(B) MSigDB Canonical Pathways enrichment analysis for the hypoxia-responsive genes in liver of WT and *Per1,2*$^{-/-}$ mice (hypergeometric test, p-value<0.05, q-value<0.2; white indicates a non-significant enrichment in the specific cell). See Dataset S8 for extra details.

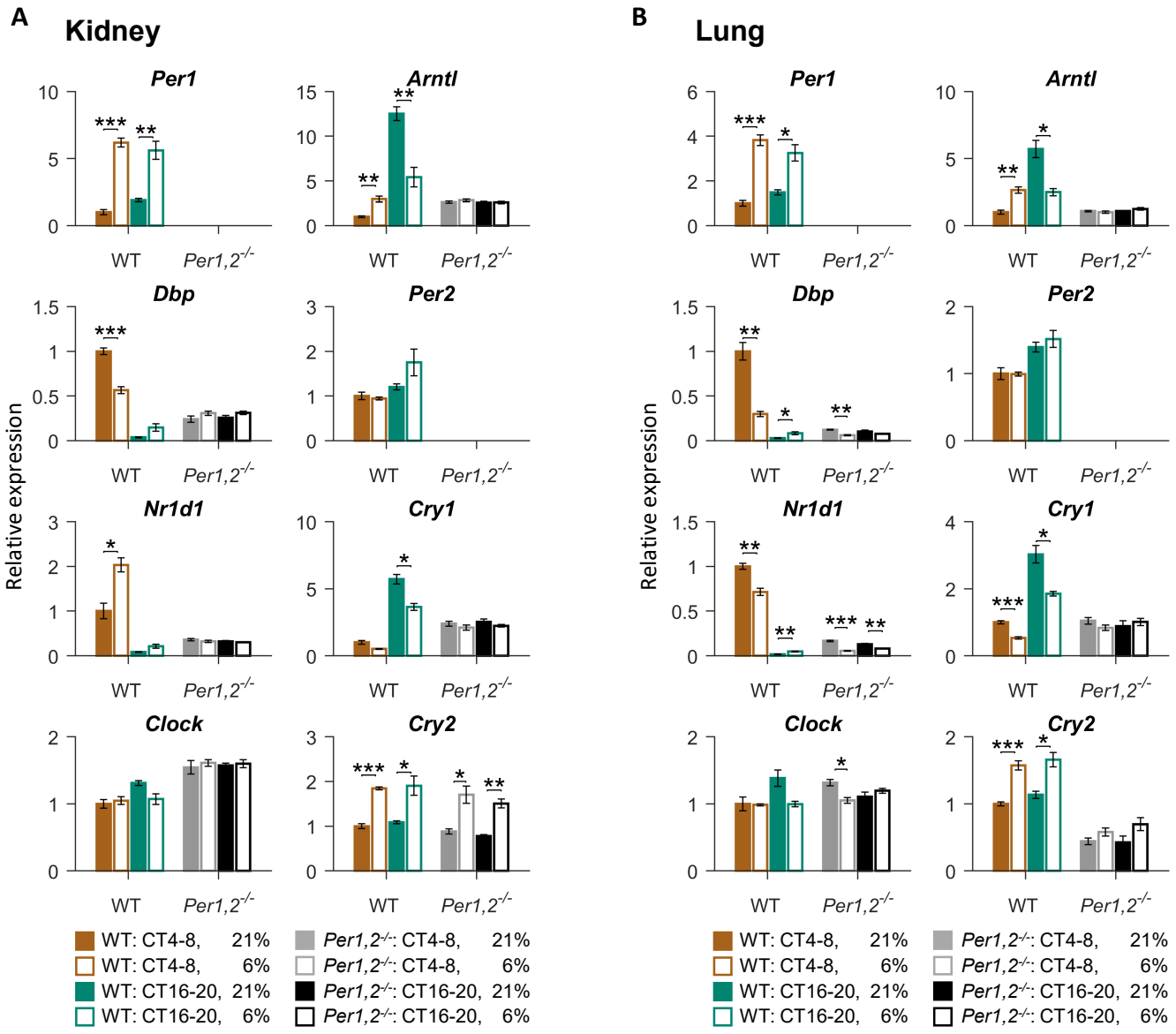
A
Kidney
B
Lung
Per1
Arntl
Dbp
Per2
Nr1d1
Cry1
Clock
Cry2
Relative expression
WT
Per1,2-/-
WT: CT4-8, 21%
WT: CT4-8, 6%
WT: CT16-20, 21%
WT: CT16-20, 6%
Per1,2-/-: CT4-8, 21%
Per1,2-/-: CT4-8, 6%
Per1,2-/-: CT16-20, 21%
Per1,2-/-: CT16-20, 6%

Figure S4. The time-dependent response to hypoxia of kidney and lung clock genes is circadian clock controlled.

Quantitative PCR analysis of clock-associated transcript levels in kidneys **(A)** and lungs **(B)** of WT or *Per1,2*$^{-/-}$ mice housed in constant dark and exposed to hypoxia (6% O_2) or normoxia (21% O_2), at the respective light (CT4-8) or dark phase (CT16-20); (mean±SE, n=4 per condition; *P<0.05, **P<0.01, ***P<0.001, two-sample Student's t-test)

A

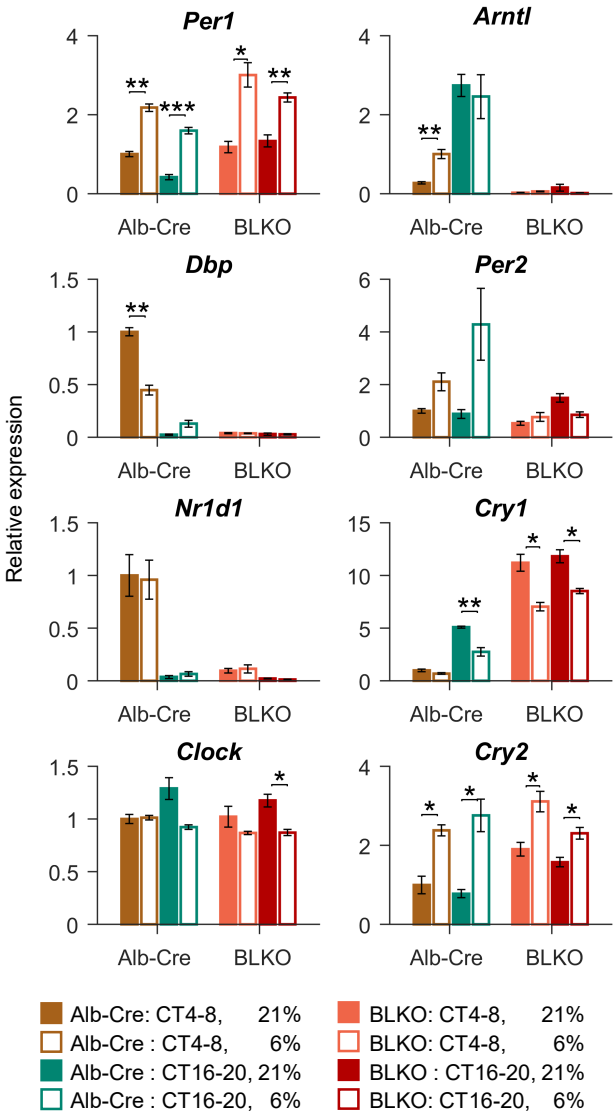
Per1
Arntl
Dbp
Per2
Nr1d1
Cry1
Clock
Cry2
Relative expression
Alb-Cre
BLKO
Alb-Cre: CT4-8, 21%
Alb-Cre : CT4-8, 6%
Alb-Cre : CT16-20, 21%
Alb-Cre : CT16-20, 6%
BLKO: CT4-8, 21%
BLKO: CT4-8, 6%
BLKO : CT16-20, 21%
BLKO: CT16-20, 6%

B

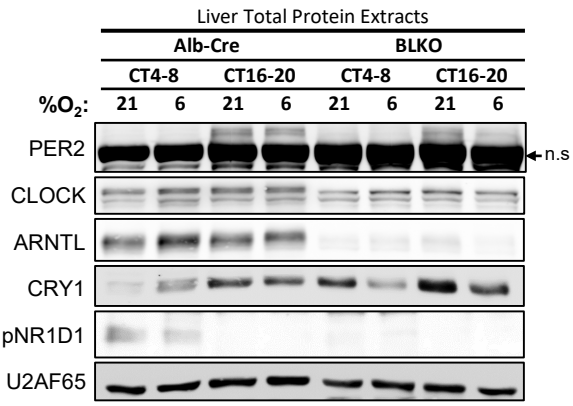
Liver Total Protein Extracts
Alb-Cre
BLKO
CT4-8
CT16-20
CT4-8
CT16-20
%O2:
21 6 21 6 21 6 21 6
PER2
n.s
CLOCK
ARNTL
CRY1
pNR1D1
U2AF65

Figure S5. The time-dependent response of liver core clock genes to hypoxia is dependent on the liver intrinsic clock.

(A) Quantitative PCR analysis of clock-associated transcript levels in livers of Alb-Cre or *Bmal1* Liver-specific Knock-Out (BLKO) mice in constant dark under normoxia (21% O_2) or hypoxia (6% O_2), at the respective light (CT4-8) or dark phase (CT16-20); (mean±SE, n=3 per condition; *P<0.05, **P<0.01, ***P<0.001, two-sample Student's t-test. *Arntl* primers are specific to exon 8, to validate the Cre cleavage).

(B) Immunoblot analysis of total liver protein extracts from Alb-Cre or BLKO mice as in (**A**), (pools of n=3; n.s., non-specific band).

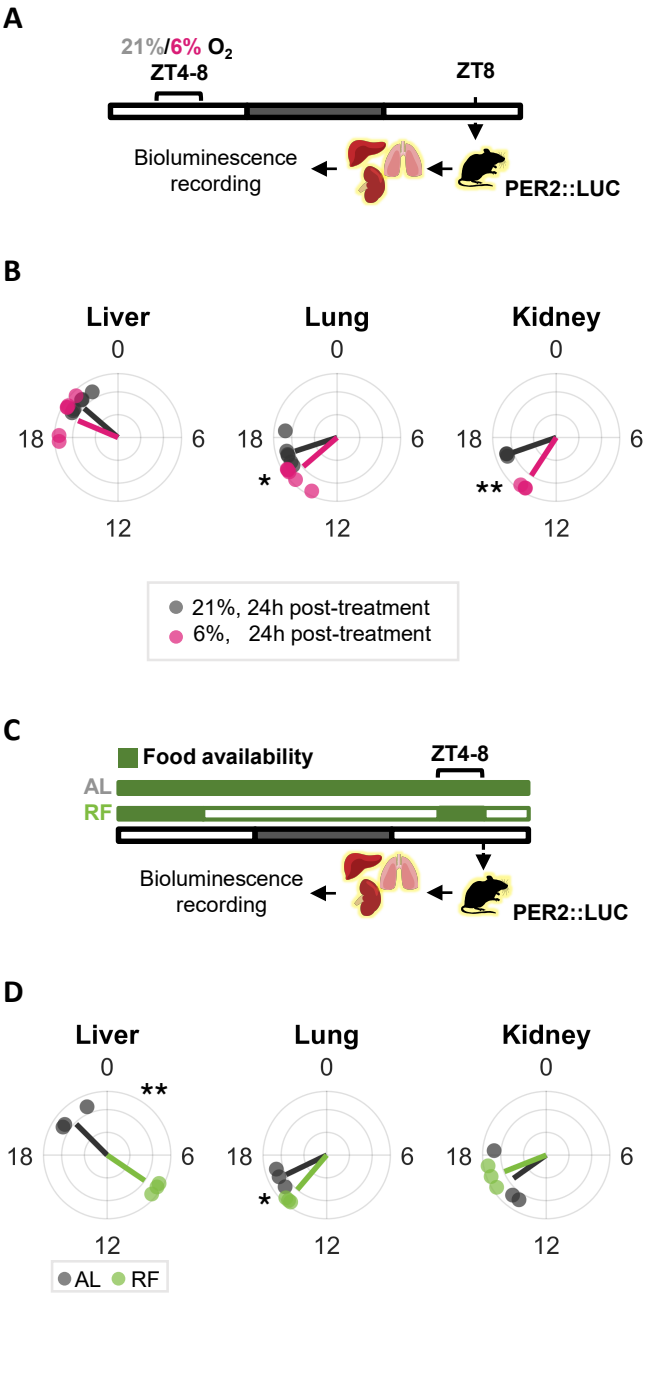
A
21%/6% O2
ZT4-8
ZT8
Bioluminescence recording
PER2::LUC
B
Liver
Lung
Kidney
0
6
12
18
*
**
21%, 24h post-treatment
6%, 24h post-treatment
C
Food availability
ZT4-8
AL
RF
Bioluminescence recording
PER2::LUC
D
Liver
Lung
Kidney
**
*
AL
RF

Figure S6. Hypoxia and restricted feeding treatments elicit inter-tissue misalignment.

(A) PER2::LUC mice were exposed to 4 h of either hypoxia (6% O_2) or normoxia (21% O_2), at the light phase (ZT4-8) and then housed in ambient air for 24 h. Animals were sacrificed and tissues harvested and sliced for bioluminescence recordings.

(B) Polar plot of the phase distribution of mice harvested 24 h following hypoxia or normoxia (n=6 for liver and lung, n=3 for kidney, *P < 0.05, **P < 0.01, Watson-Williams test).

(C) PER2::LUC mice were either fed *ad libitum* (AL) or had access to food (RF) only for 4 h (ZT4-8). Animals were sacrificed and tissues harvested and sliced for bioluminescence recordings.

(D) Polar plot of the phase distribution of PER2::LUC bioluminescence recordings following exposure to RF or AL for each tissue (n=3 per condition, *P< 0.05, **P< 0.01, Watson-Williams test).

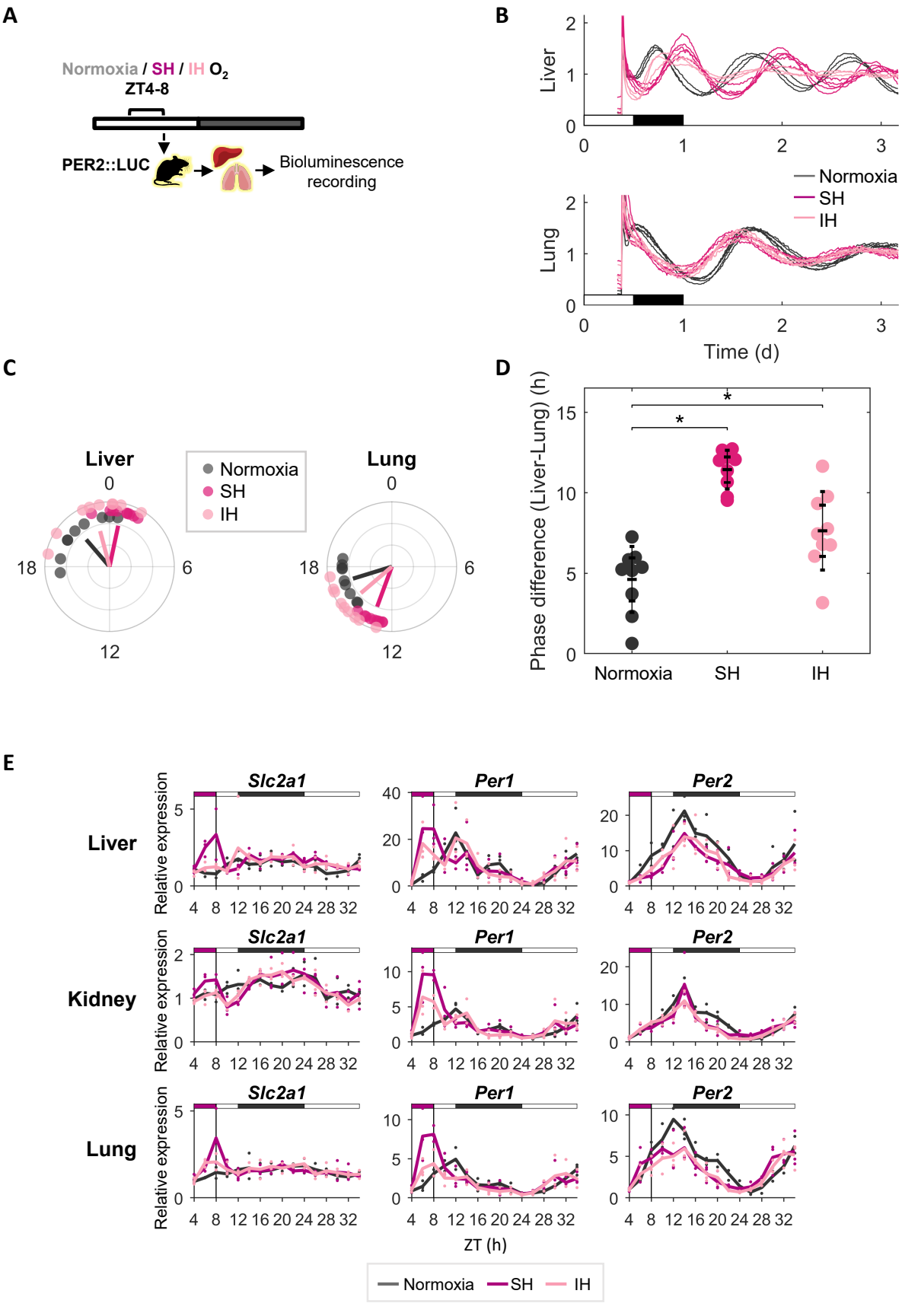
A
Normoxia / SH / IH O_2
ZT4-8
PER2::LUC
Bioluminescence recording
B
Liver
Lung
Normoxia
SH
IH
Time (d)
C
Liver
Lung
Normoxia
SH
IH
0
6
12
18
D
Phase difference (Liver-Lung) (h)
Normoxia
SH
IH
E
Liver
Kidney
Lung
Slc2a1
Per1
Per2
Relative expression
ZT (h)
Normoxia
SH
IH

Figure S7. Sustained and intermittent hypoxia elicit inter-tissue circadian clock desynchrony.

PER2::LUC mice were exposed to 4 h of either sustained hypoxia (SH; 6% O_2), intermittent hypoxia (IH) or normoxia (21% O_2), at the light phase (ZT4-8). Animals were sacrificed, tissues harvested and sliced for bioluminescence recordings.

(A) Representative relative-bioluminescence plots of organotypic slices from mice exposed to sustained, intermittent hypoxia, or normoxia control (n=1 per condition, 3-5 slices from each mouse are shown).

(B) Polar plot of the phase distribution of PER2::LUC bioluminescence recordings following exposure to sustained, intermittent hypoxia, or normoxia for each tissue (n=9 per condition).

(C) The phase difference between the liver and the lung in each of the conditions (*P<0.05, unequal variance t-test).

(D) Quantitative PCR analysis of additional transcripts from the experiment presented in Fig. 6.

Supplementary Tables

Table S1. Quantitative PCR primers

Gene	Sequences
Tbp	Forward primer 5'-CCCTATCACTCCTGCCACACCAGC-3'
	Reverse primer 5'-GTGCAATGGTCTTTAGGTCAAGTTTACAGCC-3'
Rplp0	Forward primer 5'- AGATTCGGGATATGCTGTTGGC-3'
	Reverse primer 5'- TCGGGTCCTAGACCAGTGTTC-3'
Clock	Forward Primer 5'- AGAACTTGGCATTGAAGAGTCTC-3'
	Reverse Primer 5'- GTCAGACCCAGAATCTTGGCT-3'
Arntl	Forward Primer 5'-CCAAGAAAGTATGGACACAGACAAA-3'
	Reverse Primer 5'-GCATTCTTGATCCTTCCTTGGT-3'
	Probe 5'-FAM-TGACCCTCATGGAAGGTTAGAATATGCAGAA-TAMRA-3'
Nr1d1	Forward Primer 5'-TGCAGGCTGATTCTTCACACA-3'
	Reverse Primer 5'-AGCCCTCCAGAAGGGTAGGA-3'
	Probe 5'-FAM-ACACTCTCTGCTCTTCCCATGCAAATCAG-TAMRA-3'
Per1	Forward primer 5'-ACCAGCCATTCCGCCTAAC-3'
	Reverse primer 5'-CGGGGAGCTTCATAACCAGA-3'
Per2	Forward Primer 5'-ATGCTCGCCATCCACAAGA-3'
	Reverse Primer 5'-GCGGAATCGAATGGGAGAAT-3'
	Probe 5'-FAM-ATCCTACAGGCCGGTGGACAGCC-TAMRA-3'
Cry1	Forward Primer 5'-CACTGGTTCCGAAAGGGACTC-3'
	Reverse Primer 5'- CTGAAGCAAAAATCGCCACCT-3'
Cry2	Forward Primer 5'- CACTGGTTCCGCAAAGGACTA-3'
	Reverse Primer 5'- CCACGGGTCGAGGATGTAGA-3'
Dbp	Forward Primer 5'- TGGCCCGAGTCTTTTTGC-3'
	Reverse Primer 5'- GCGTCCAGGTCCACGTATTC-3'
	Probe 5'-FAM- CCGCTGCTGTGGGAACGCACT-TAMRA-3'
Slc2a1	Forward primer 5'- CAGTTCGGCTATAACACTGGTG-3'
	Reverse primer 5'- GCCCCCGACAGAGAAGATG-3'
Pdk1	Forward primer 5'- GGACTTCGGGTCAGTGAATGC-3'
	Reverse primer 5'- TCCTGAGAAGATTGTCGGGGA-3'
Ldhα	Forward primer 5'- TGTCTCCAGCAAAGACTACTGT-3'
	Reverse primer 5'- GACTGTACTTGACAATGTTGGGA-3'
Epo	TaqMan Mm00433126 (ThermoFisher)
Egln3	Forward primer 5'- AGGCAATGGTGGCTTGCTAT-3'
	Reverse primer 5'- GACCCCTCCGTGTAACTTGG-3'
Arntl (exon 8)	Forward primer 5' – GACCTACTCTCCGGTTCCCT-3'
	Reverse primer 5'- ATTTTGTCCCGACGCCTCTT-3'

Supplementary Datasets Legends

Dataset S1.xlsx: RNA-seq results: LD (Liver, Kidney and Lung)

Rows correspond to genes (at least 2 counts in at least 2 samples). Columns: “sample_name.raw” – raw counts; “sample_name.norm” – normalized counts; “P.padjScreen” – FDR for the screening hypothesis; “P.ZT8rsp”– adjusted p-values for the response to hypoxia at ZT8; ”P.ZT20rsp” – adjusted p-values for the response to hypoxia at ZT20; ”P.Basal” – adjusted p-values for the basal time effect; "P.Inter" – adjusted p-values for the interaction (time-dependent hypoxia effect); "padjScreen","ZT8rsp","ZT20rsp","Basal","Inter” – 1 if pass (P<0.05) for the indicated comparison, 0 if not; "LFC.ZT8rsp","LFC.ZT20rsp","LFC.Basal","LFC.Inter" – the Log2 of the fold-change between the compared conditions. Same notation is used for Dataset S2.

Dataset S2.xlsx: RNA-seq results: Liver DD wild-type (WT) and *Per1,2*$^{-/-}$

Dataset S3.xlsx: Lists of hypoxia responsive genes in each tissue

Dataset S4.xlsx: Lists of time-dependent responsive genes in each tissue

Dataset S5.xlsx: Lists of hypoxia responsive genes in wild-type and Per1,2$^{-/-}$ livers

Dataset S6.xlsx: Lists of basal-time changing genes in wild-type and Per1,2$^{-/-}$ livers

Dataset S7.xlsx: Motif enrichment analysis results

Dataset S8.xlsx: MSigDB Canonical Pathways enrichment results

Tab A: for liver, kidney and lung in response to hypoxia at ZT8 or ZT20

Tab B: for wild-type or *Per1,2*$^{-/-}$ livers in response to hypoxia

Rows correspond to gene sets (pathways from the MSigDB) significantly enriched in each experimental group of genes ("Condition"). "Pathway" – the MSigDB gene set name; "GeneRatio" – the pathway members out of the experimental group; "BgRatio" – the total pathway size out of the reference genome size; "pvalue" – the hypergeometric test p-value; "qvalue" – the FDR of the p-value; "geneID" – the pathway members present in the experimental group; "Count" – the number of pathway members present in the experimental group. Same notation is used for Tab **B**.

SI References

1. Zheng B, *et al.* (2001) Nonredundant roles of the mPer1 and mPer2 genes in the mammalian circadian clock. *Cell* 105(5):683-694.
2. Yoo SH, *et al.* (2004) PERIOD2::LUCIFERASE real-time reporting of circadian dynamics reveals persistent circadian oscillations in mouse peripheral tissues. *Proc Natl Acad Sci U S A* 101(15):5339-5346.
3. Storch KF, *et al.* (2007) Intrinsic circadian clock of the mammalian retina: importance for retinal processing of visual information. *Cell* 130(4):730-741.
4. Jaitin DA, *et al.* (2014) Massively parallel single-cell RNA-seq for marker-free decomposition of tissues into cell types. *Science* 343(6172):776-779.
5. Kohen R, *et al.* (2019) UTAP: User-friendly Transcriptome Analysis Pipeline. *BMC Bioinformatics* 20(1):154.
6. Martin M (2011) Cutadapt removes adapter sequences from high-throughput sequencing reads. *2011* 17(1):3.
7. Dobin A, *et al.* (2013) STAR: ultrafast universal RNA-seq aligner. *Bioinformatics* 29(1):15-21.
8. Anders S, Pyl PT, & Huber W (2015) HTSeq--a Python framework to work with high-throughput sequencing data. *Bioinformatics* 31(2):166-169.
9. Robinson MD, McCarthy DJ, & Smyth GK (2010) edgeR: a Bioconductor package for differential expression analysis of digital gene expression data. *Bioinformatics* 26(1):139-140.
10. Van den Berge K, Soneson C, Robinson MD, & Clement L (2017) stageR: a general stage-wise method for controlling the gene-level false discovery rate in differential expression and differential transcript usage. *Genome Biol* 18(1):151.
11. Ritchie ME, *et al.* (2015) limma powers differential expression analyses for RNA-sequencing and microarray studies. *Nucleic Acids Res* 43(7):e47.
12. Korotkevich G, Sukhov V, & Sergushichev A (2019) Fast gene set enrichment analysis. *bioRxiv*:060012.
13. Subramanian A, *et al.* (2005) Gene set enrichment analysis: a knowledge-based approach for interpreting genome-wide expression profiles. *Proc Natl Acad Sci U S A* 102(43):15545-15550.
14. Liberzon A, *et al.* (2011) Molecular signatures database (MSigDB) 3.0. *Bioinformatics* 27(12):1739-1740.
15. Xie X, *et al.* (2005) Systematic discovery of regulatory motifs in human promoters and 3' UTRs by comparison of several mammals. *Nature* 434(7031):338-345.
16. Yu G, Wang LG, Han Y, & He QY (2012) clusterProfiler: an R package for comparing biological themes among gene clusters. *OMICS* 16(5):284-287.
17. Durinck S, Spellman PT, Birney E, & Huber W (2009) Mapping identifiers for the integration of genomic datasets with the R/Bioconductor package biomaRt. *Nat Protoc* 4(8):1184-1191.
18. Aviram R, *et al.* (2016) Lipidomics Analyses Reveal Temporal and Spatial Lipid Organization and Uncover Daily Oscillations in Intracellular Organelles. *Mol Cell* 62(4):636-648.

19. Lavery DJ & Schibler U (1993) Circadian transcription of the cholesterol 7 alpha hydroxylase gene may involve the liver-enriched bZIP protein DBP. *Genes Dev* 7(10):1871-1884.
20. Berens P (2009) CircStat: A MATLAB Toolbox for Circular Statistics. *J Stat Softw* 31(10):1-21.